Methodology for Analysing the NOx-NH3 Trade-off for the Heavy-duty Automotive SCR Catalyst

Åberg, Andreas; Widd, Anders; Abildskov, Jens; Huusom, Jakob Kjøbsted

Published in:
IFAC-PapersOnLine

Link to article, DOI:
10.1016/j.ifacol.2017.08.1435

Publication date:
2017

Document Version
Publisher's PDF, also known as Version of record

Available online at www.sciencedirect.com

ScienceDirect

IFAC Papers Online CONFERENCE PAPER ARCHIVE

IFAC PapersOnLine 50-1 (2017) 5998–6003

Methodology for Analysing the NOx-NH_3 Trade-off for the Heavy-duty Automotive SCR Catalyst

Andreas Åberg * **Anders Widd** ** **Jens Abildskov** * **Jakob K. Huusom** *

* *CAPEC-PROCESS Research Centre, Department of Chemical and Biochemical Engineering, Tehcnical University of Denmark, Søltofts Plads, Building 229, DK-2800 Kgs. Lyngby, Denmark*
** *Haldor Topsoe A/S, Haldor Topsøes Allé 1, DK-2800 Kgs. Lyngby, Denmark*

Abstract: This paper presents a methodology where pareto fronts were used to analyse how changes in the control structure for the urea dosing to the automotive SCR catalyst can improve the trade-off between NOx slip and NH_3 slip. A previously developed simulation model was used to simulate the European Transient Cycle (ETC) with P, PI, PD, and PID controllers, combined with Ammonia-NOx-Ratio (ANR) based feedforward to control the urea dosing. Results showed that PI with feedforward performed best. It was also shown that combining feedback with feedforward performed better than only using feedback or feedforward.

Keywords: Automotive control, Automotive emissions, SCR, PID control, Feedback control, Feedforward control, Pareto front.

1. INTRODUCTION

1.1 Background

Diesel engine exhaust gases contains several harmful substances. The main pollutants are carbon monoxide (CO), hydrocarbons (HC), particulate matter (PM), and nitrous gases such as nitrogen oxide (NO) and nitrogen dioxide (NO_2) (together NO_x). Reducing the emission of these pollutants is of great importance due to their effect on urban air quality, and because of new legislations (Fritz and Pitchon, 1997; R.M. Heck and R.J. Farrauto, 2001). In a modern EU VI exhaust gas treatment system for heavy duty applications, the exhaust gases are typically treated with four different catalysts: a Diesel Oxidation Catalyst (DOC) which oxidises HC and CO to H_2O and CO_2, and NO to NO_2, a Diesel Particulate Filter (DPF) which filters PM, a Selective Catalytic Reduction (SCR) catalyst which removes NO and NO_2, and an Ammonia Slip Catalyst (ASC) which removes excess ammonia (NH_3) before the gases are released to the atmosphere. A representation of the system and the effect each catalyst has on the composition can be seen in Figure 1. A promising and widely used technology for removing NOx is based on SCR, with NH_3 in the form of hydrolyzed urea as a reducing agent (P. Gabrielsson, 2004). Challenges with this technology include dosing the appropriate amount of urea to reach sufficient NO_x conversion, while at the same time keeping NH_3-slip from the exhaust system below the legislation. This requires efficient control. Closed loop control of the SCR catalyst has been studied extensively in literature (C. Schär et al., 2004; J. Hu et al, 2011; D. Y. Wang et al, 2008), and feedforward based controllers (J. Patchett et al., 2003; D. Seher et al., 2003). Problems with feedback control are for example cross-sensitivity of NH_3 in NOx-sensors, dynamics with greatly varying time constants in combination with a transient system, and time delay in the urea dosing system (F. Willems et al., 2007). The exhaust systems rarely has NH_3 sensors, making it difficult to use NH_3 based control.

The performance measure of a controller is its ability to meet the legislation. However if a controller meets legislation, it is difficult to compare controllers against each other. Due to the nature of the SCR catalyst, the evaluation is a trade-off between NOx slip and NH_3 slip. Contributions in literature often focus on optimising a single control structure for a given system, rather than a full analysis of how different control structures can improve the performance of the SCR catalyst. Using pareto fronts to graphically analyse the best possible trade-off between NOx slip and NH_3 slip for a given control structure, and how the trade-off can be improved by changing the control structure, can to the author's knowledge not be found in literature.

1.2 Contribution

This paper presents a methodology to graphically analyse the trade-off between NOx slip and NH_3 slip for the automotive SCR catalyst. The methodology can be used to investigate how changes in the urea dosing control structure improves the trade-off performance. Pareto fronts are generated for P, PI, PD, and PID controllers, both with and without ANR based feedforward, by simulating the European Transient Cycle (ETC) with the model by Åberg et al (A. Åberg et al., 2016b). The performance gain or loss for different control structures is analysed graphically.

10.1016/j.ifacol.2017.08.1435

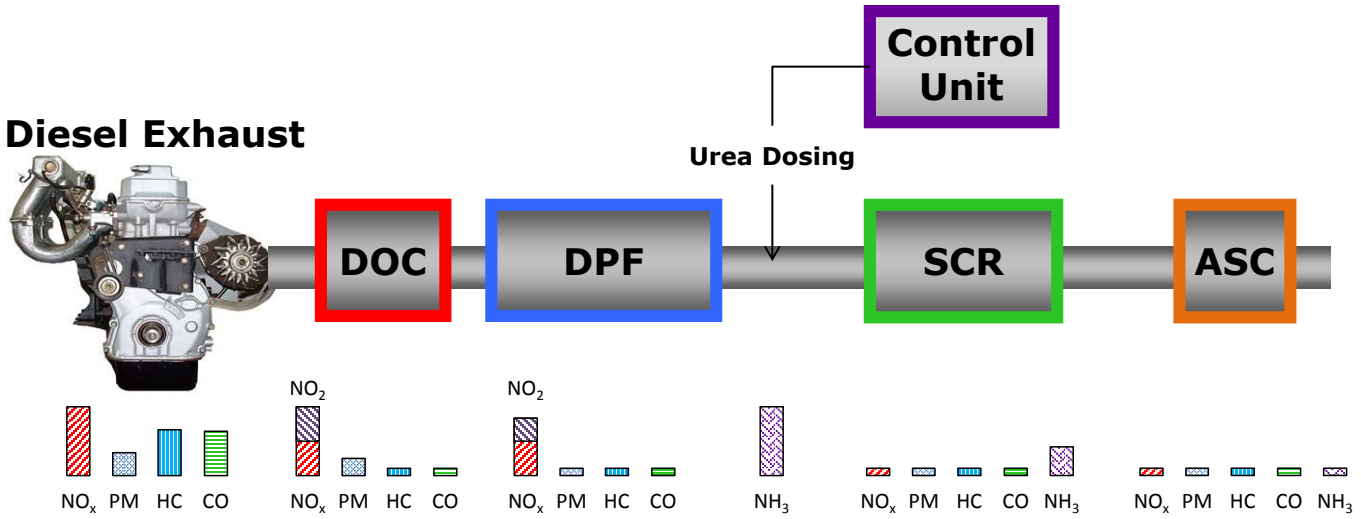

Fig. 1. The standard Euro VI diesel engine exhaust gas cleaning system. The bars below the catalysts represent the effect each catalyst has on exhaust gas composition.

1.3 Outline

Section 2 describes the developed methodology, and the tools used to produce the pareto fronts. Section 3 presents results where the methodology is applied to P, PI, PD and PID controllers, both with and without feedforward. Section 4 presents a discussion about implications of the results and how the methodology can be used. Conclusions are drawn in section 5.

2. METHODOLOGY

This section will present the simulation model that has been used to generate pareto fronts for the analysed controllers. The tested controllers will be presented together with the methodology to generate the pareto fronts.

2.1 Simulation Model

The simulation model that was used to simulate the process with different controllers can be found in (A. Åberg et al., 2016a,b). The model is based on first principles and has been shown to predict the output during transient cycles adequately. The model considers the following reactions:

$$\mathrm{NH_3 + S \leftrightharpoons S - NH_3} \quad (1)$$

$$\mathrm{2S - NH_3 + 5/2O_2 \rightarrow 2NO + 3H_2O + 2S} \quad (2)$$

$$\mathrm{4S - NH_3 + 4NO + O_2 \rightarrow 4N_2 + 6H_2O + 4S} \quad (3)$$

$$\mathrm{2S - NH_3 + NO + NO_2 \rightarrow 2N_2 + 3H_2O + 2S} \quad (4)$$

$$\mathrm{2S - NH_3 + 2NO_2 \rightarrow N_2 + N_2O + 3H_2O + 2S} \quad (5)$$

where S represents an empty catalyst adsorption site for NH_3. S-NH_3 represents an adsorbed NH_3 molecule. The model can thus be used to analyse the NOx-NH_3 trade-off. The model has been validated by simulating a full-scale SCR monolith with engine gases from the ETC. A NH_3 slip catalyst was not simulated after the SCR catalyst, meaning that the NH_3 emissions would be lower in a real system than what is presented here. The simulated catalyst had a volume of 18.7 L, meaning that it was designed to meet EURO V emission limits. The emission inputs were generated experimentally by running the ETC on a 11 L diesel engine.

2.2 Controllers

P, PI, PD, and PID controllers have been tested both with and without feedforward action. The feedforward action throughout this article is referring to NOx inlet measurement based feedforward, as in (6),

$$u^{FF} = \mathrm{ANR} \cdot \mathrm{NOx}_{in} \quad (6)$$

where u^{FF} is the calculated feedforward dosing, ANR is the predetermined Ammonia-NOx-Ratio, and NOx_{in} is the inlet NOx concentration. The controllers that have been tested can be formulated as

$$u(t_k) = K_c \left(e(t_k) + \frac{T_s}{T_i} \sum_{t=1}^{T} e(t_k) + D(t_k) \right) + u^{FF}(t_k) \quad (7)$$

where $u(t_k)$ is the dosing of NH_3 in mol/m^3 at time t_k, K_c is the gain, T_i is the integral time, T is the time the cycle has been running, subscript k indicates the time, T_s is the sampling time, $e(t_k)$ is

$$e(t_k) = r - NOx_{conversion}(t_k), \quad (8)$$

where r is the set point in NOx conversion, and $D(t_k)$ is the derivative action given by (K. J. Åström and M. Murray, 2008)

$$D(t_k) = \frac{T_d}{T_d + NT_s} D(t_{k-1}) - \frac{T_d N}{T_d + NT_s} (e(t_k) - e(t_{k-1})) \quad (9)$$

where T_d is the derivative time, and N is the filtering factor. The expression in (7) represents all controllers that have been tested in this work. A P controller represents the scenario where $T_i \rightarrow \infty$, $T_d = 0$, and ANR $= 0$. A PI controller is the case where $T_d = 0$, and ANR $= 0$. A PD controller is when $T_i \rightarrow \infty$ and ANR $= 0$. A controller coupled with feedforward is the case where ANR > 0, and the same parameters as previously. The sampling time T_s was 1s. The set point r was set to 100 % conversion in all simulations.

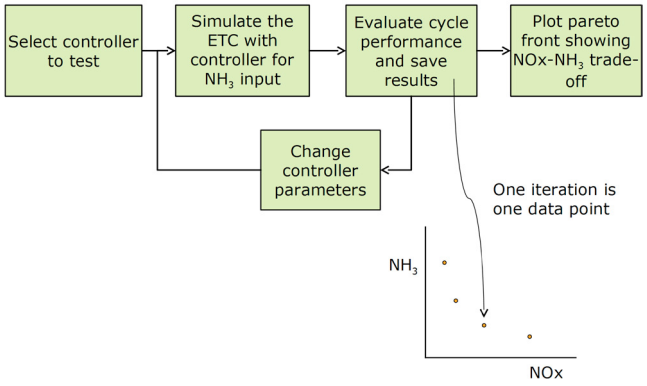

Fig. 2. Procedure to generate the pareto fronts.

In this work the feedback was based on only NOx conversion, as seen in eq.(8). As stated in section 1, a problem with NOx sensor based control is that the sensors are cross-sensitive to NH_3. This effect was not taken into consideration, and the sensors were considered to be noise-free. This was done because the objective of this work was to analyse the difference in performance between ideal controllers using the developed methodology.

It was assumed that the dosing was instant and was uniformly distributed to the catalyst. It was also assumed that the urea was decomposed instantly to NH_3. These assumptions will likely have an impact compared to the real application, where dosing delay and urea decomposition are problems (F. Willems et al., 2007), however the general trends of the pareto fronts will be the same.

2.3 Pareto Fronts

The control problem in SCR monoliths is of a multi-objective nature due to the legislation which places limits on NOx slip, average NH_3 slip, and maximum NH_3 slip. The set of solutions to a multi-objective optimisation problem can be represented as a pareto front, which is the curve representing the solutions that are pareto efficient. Here, pareto fronts were used to present the trade-off between NOx slip and NH_3 slip for different controllers. The process of producing the pareto fronts is shown in Figure 2. A controller is selected for testing, for example a P controller. The ETC is simulated using the controller with a certain K_c parameter. The cycle performance is evaluated, and the results are saved. This represents one data point on the pareto front. The process is repeated with a new K_c parameter, until a pareto front is complete. For controllers that have several parameters, such as a PI controller, the pareto fronts were generated using the same procedure, but for a certain T_i. A range of T_i values were tested and pareto fronts for each T_i were produced by simulating the cycle for a range of K_c values, and the influence of T_i was therefore evaluated. The parameter values for K_c, T_i, and T_d that has been used are based on values that gave reasonable performance. The performance was evaluated using the NOx slip in g/kWh for the entire cycle, and the average NH_3 slip in vol-ppm. The NOx mass was calculated by assuming that all NOx is NO_2. The average NH_3 slip was calculated by taking the mean of all NH_3 outlet concentration measurements. After the pareto fronts are generated a visual representation of the tested configurations of a control structure is achieved. This can be used to see which controller satisfies the legislations. It also enables comparisons between controllers, as it becomes clear if a control structure outperforms another structure. The benefit of the analysis is that the conclusions on control structure should be independent of the size or activity of the monolith. The qualitative results should also be independent on parameters such as engine size, and ambient conditions. The pareto fronts are in most cases cropped, to present relevant results. The pareto fronts presented here have a higher NH_3 slip and lower NOx slip than is typical for a monolith of this size. This is done because the differences between the controllers is more clear at lower NOx slip, and the qualitative results remain the same.

The commercial software Matlab was used for simulation. The simulated monolith was a full body vanadium based catalyst with 270 CPSI on a corrugated substrate, 12.7 inches long and 9 inches diameter. The engine was a 10 liter engine without EGR, following the ETC. For each pareto front 40 simulations were performed, where each took approximately 500 s. The initial conditions for each simulation was the end result of the previous simulation. For the first simulation in a series, the simulation was performed twice to achieve realistic initial conditions.

3. RESULTS AND DISCUSSION

This section will present the pareto fronts for P, PI, PD, and PID controllers, both with and without feedforward.

3.1 P-control

The P controller has one free parameter, the gain K_c. Figure 3 shows the pareto fronts for P controllers with varying degrees of feedforward, ranging from ANF = 0 to ANF = 1.5. It can be seen that the controller with ANR = 0 starts to increase in average NH_3 slip rapidly after the NOx slip goes below 3 g/kWh. The EURO IV emission limited the NOx slip to 3.5 g/kWh, and it appears that a P controller was enough to meet the previous emission limits, atleast with the assumptions included in this work. As the feedforward is increased it can be seen that the pareto front is shifted inwards, giving a better trade-off between NOx and NH_3. When ANR > 1, meaning that more NH_3 than NOx is dosed, the pareto fronts are shifted upwards, and the feedforward that should be used depends on the required NOx slip.

3.2 PI-control

The PI controller has two free parameters, the gain K_c and the integral time T_i. Figure 4 shows the influence of the integral time for a PI controller without any feedforward. As seen, the difference in the cycle based performance for different T_i is small. The transient ETC ensures that the process is never in steady state, and it makes little difference if the integral action is acting towards a hypothetical steady state in 60s or 70s. Figure 5 shows the pareto fronts for a PI controller with ANR = 0, and ANR = 0.9-1.2. It can be seen that as with the P controller, introducing feedforward improves performance. The overlap between controllers when the feedforward is increased

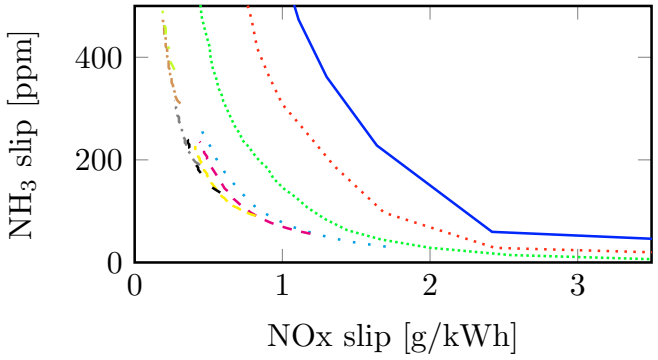

Fig. 3. Pareto fronts for simulated P controllers with the ETC, with different levels of ANR feedforward. Legend: ANR = 0 (——), ANR = 0.2 (·····), ANR = 0.5 (·····), ANR = 0.8 (· · · ·), ANR = 0.9 (– – –), ANR = 1.0 (– · – ·), ANR = 1.1 (– – –), ANR = 1.2 (– · · –), ANR = 1.4 (– · · –), ANR = 1.5 (– · – ·)

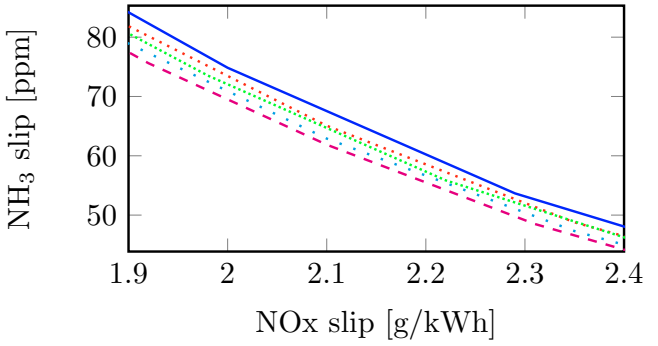

Fig. 4. Pareto fronts for simulated PI controllers with the ETC, with different integral times. Legend: $T_i = 40$ (——), $T_i = 50$ (·····), $T_i = 60$ (·····), $T_i = 70$ (· · · ·), $T_i = 80$ (– – –)

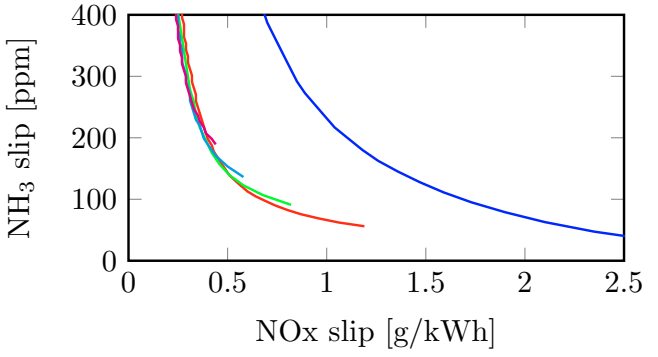

Fig. 5. Pareto fronts for simulated PI controllers with the ETC, with different levels of ANR feed forward. The integral time for all simulation was $T_i = 70$. Legend: ANR = 0 (——), ANR = 0.9 (——), ANR = 1.0 (——), ANR = 1.1 (——), ANR = 1.2 (——)

is more prominent with the PI controller than with the P controller. Generally it seems better to increase the K_c parameter up to a certain level, instead of increasing the feedforward. When the feedback becomes too strong, increasing the feedforward is better for the NOx-NH_3 trade-off. The trade-off curves become increasingly steep as feedforward is increased, which is also seen with the P

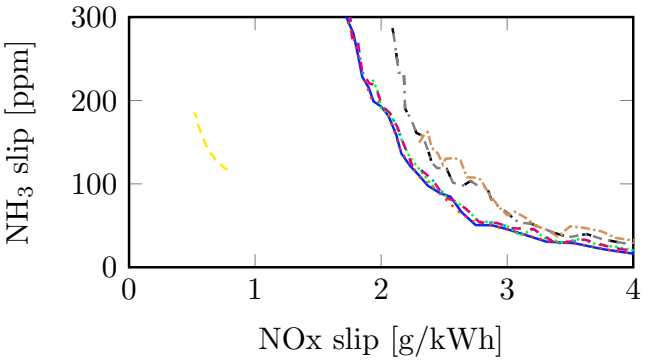

Fig. 6. Simulated PD controllers with the ETC, with different T_d and N. Legend: $T_d = 0.5$, $N = 15$ (——), $T_d = 0.5$, $N = 20$ (·····), $T_d = 1$, $N = 10$ (·····), $T_d = 1$, $N = 15$ (· · · ·), $T_d = 10$, $N = 10$ (– – –), $T_d = 10$, $N = 20$ (– · – ·), $T_d = 12$, $N = 20$ (– · · –), $T_d = 15$, $N = 15$ (– · · –), $T_d = 1$, $N = 15$, ANR = 1.0 (– · – ·)

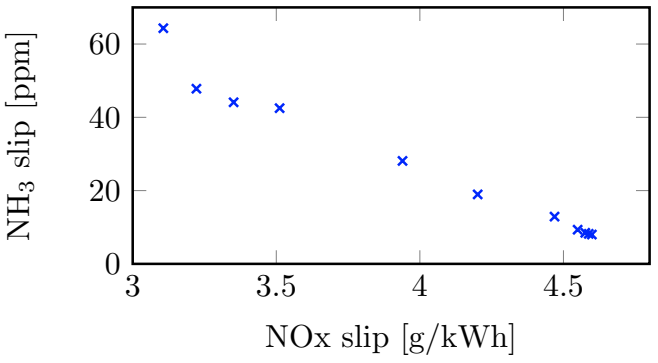

Fig. 7. Erratic behaviour for PD controllers when the gain K_c is kept constant and the derivative time T_d is increased.

controller. This is likely because of fundamental limits of the control structure, and the NOx slip can not become smaller than a certain limit. At ANR = 1.2 and beyond, increasing the feedback only gives an increase in NH_3 slip, while not reducing the NOx slip.

3.3 PD-control

The PD controller has three free parameters, the gain K_c, the derivative time T_d, and the filtering factor N. Figure 6 shows several pareto fronts with different T_d and N parameters. As can be seen the curves have an erratic shape and for a given T_d and N, two different K_c can give the same NH_3 slip and different NOx slip. (K. J. Åström and M. Murray, 2008) state that the N parameter normally takes values between 8 and 20, which has been adopted here. The derivative time has also been tested in a broad range, with limited success. The PD controller performs worse than P controllers that were shown in Figure 3. To investigate if the reason for the erratic shape was a too strong derivative action, the gain was held constant while increasing the derivative time, in Figure 7.

It can be seen that even for low derivative times, the trade-off curve became irregular and no smooth shape

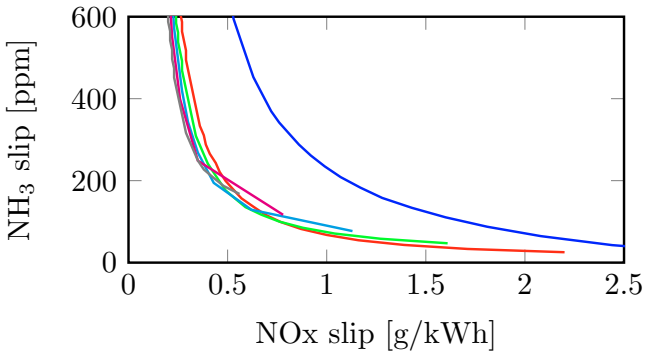

Fig. 8. Simulated PID controllers with the ETC, with different levels of ANR feed forward. Legend: ANR = 0 (——), ANR = 0.7 (——), ANR = 0.8 (——), ANR = 0.9 (——), ANR = 1.0 (——), ANR = 1.1 (——)

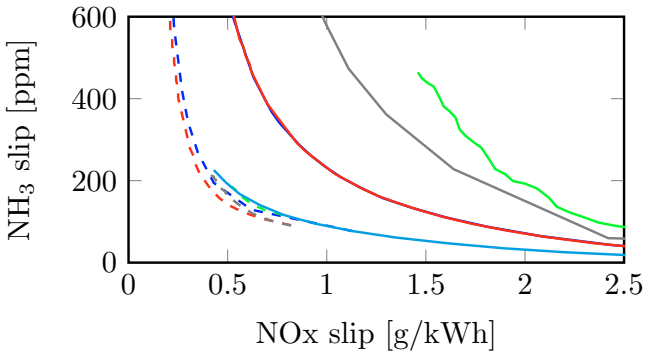

Fig. 9. Simulated PID controllers with the ETC, with different levels of ANR feed forward. Legend: P (——), P with ANR = 1 (- - -), PI (——), PI with ANR = 1.0 (- - -), PD (——), PD with ANR = 1.0 (- - -), PID (——), PID with ANR = 1.0 (- - -), ANR = 0:1.0 (——)

was obtained. The reasons for this behaviour is unknown, however we suspect that even though the signal was considered noise free, the transient input resulted in a rapidly changing error, that the derivative action was sensitive to. The fact that the results showed cases where the controller gave the same NH_3 slip for different NOx-slip, suggests there are periods where one parameter set results in a large NH_3 slip at a certain time, while the other parameter set does not. Because of these results and the fact that the PD controller performed worse than a P controller even for good parameters, it was decided not to look further into these problems, and abandon the PD controller from further consideration.

3.4 PID-control

The PID controller has four free parameters, the gain K_c, the integral time T_i, the derivative time T_d, and the filtering factor N. T_i was chosen as the value that showed the best performance during PI analysis in section 3.2, and T_d and N were chosen based on performance in PD analysis in section 3.3. Figure 8 shows pareto fronts for PID controllers with ANR = 0, and ANR = 0.7-1.1. It can be seen that the negative effect of derivative action seems to have disappeared. If it is improving performance cannot be concluded until it is compared with the PI controller in section 3.5. The performance is, as with the P and PI controller, improved when feedforward is included. The overlap seen previously when feedforward is increased is also seen here.

3.5 Comparison

Figure 9 compares some of the previous results. The best controller tested was the PI with feedforward ANR = 1.0. This controller outperformed the P controller with feedforward, meaning that the integral action increased performance when combined with feedforward as well. The difference between a P controller and a PI controller was however substantially bigger without feedforward. The reason integral action improves performance even though no steady state is reached is because it ensures that there is continous dosing, even during periods of low error. The effect of feedforward was dominating, and as can be seen, a P controller with feedforward outperformed a PI controller without feedforward. The difference between a PI controller and PID controller without feedforward is difficult to see in Figure 9. However if zoomed, it can be seen that the PI controller was slightly better than the PID controller. This confirms that the derivative action has little or no effect at the expense of added complexity, also combined with other parts. Figure 9 shows that controllers including both feedback and feedforward performed better than controllers with only feedforward. This shows that even though the feedforward was dominating, the feedback control action contributes to the cycle based performance.

4. DISCUSSION

The presented methodology provides a way to compare controllers graphically in their whole operational span. Although it has only been applied to P, PI, PD, and PID controllers with feedforward in this work, it can be applied to other controllers as well, for example model based controllers, controllers based on NH_3, etc. For a controller that requires an optimisation problem to be solved, it is suitable if the user is uncertain about the weights that should be used in the objective function. If the objective function weights are changed and the solutions presented using pareto fronts, the pareto fronts will give an overview of which weights corresponds to the desired controller performance. Due to the large number of parameters that has to be tested to generate the pareto fronts, the methodology would become resource intensive if it was applied experimentally directly. It is thus more suitable for comparing controllers through simulation. The controllers and shape of the pareto fronts can be validated experimentally with a smaller number of experiments, to confirm that the same results can be achieved when dosing delay, cross sensitivity to NH_3, and other factors are considered.

In this work the pareto fronts have been based on entire-cycle based performance by measuring the average NH_3 slip and total NOx slip. The current legislation includes rules about the total NOx slip, the average NH_3 slip over the entire cycle, and the maximum NH_3 peak at any given time. The pareto fronts can be modified to

represent the maximum peak slip, or expanded so that all three legislative limits are covered. NH_3 consumption can also be included as a criteria in the optimisation problem. Addition of sensor noise or cross sensitivity can also be added to the model, thereby giving a more realistic controller performance.

The results are general in the sense that changes in catalyst volume or other system parameters would change the quantitative results but not the qualitative. This has been confirmed in simulations not shown here, where the pareto fronts for the P and PI controllers were plotted for two different volumes. As expected, the larger volume improves the trade-off between NOx slip and NH_3 slip, since more catalyst is available for reaction.

The study shows that out of the tested control structures, the feedforward is important for the overall performance. Sensors before the SCR catalyst are therefore recommended. It is possible to use an engine-NOx map that provides information about the engine outlet NOx levels for different driving conditions. This however suffers from some problems, such as not taking ambient conditions into account.

5. CONCLUSIONS

This paper has presented a methodology to analyse the trade-off between NOx slip and NH_3 slip for the automotive SCR catalyst by using pareto fronts. The methodology was applied to P, PI, PD, and PID controllers both with and without ANR-based feedforward. It was shown that the PI controller with feedforward included gave the best trade-off. It was also shown that there is a performance increase in combining feedback with feedforward compared to using either one alone.

ACKNOWLEDGEMENTS

The financial support from Innovation Fund Denmark under grant number 103-2012-3 is gratefully acknowledged.

REFERENCES

A. Fritz, V. Pitchon. The current state of research on automotive lean NOx catalysts, *Applied Catalysis B* 13, 1997, 1.

R.M. Heck, R.J. Farrauto Automobile exhaust catalysis, *Applied Catalysis A* 221, 2001, 443.

P. L. T. Gabrielsson. Urea-SCR in automotive applications, *Topics in Catalysis* 28, 2004, 1-4.

C. Schär. C. Onder, and H. Geering. Control of an SCR catalytic converter system for mobile heavy-duty application, *IEEE Transactions on Control Systems Technology*, vol. 14, no. 4, 2006, 641-653.

J. Hu, Y. Zhao, Y. Zhang, S. Shuai, and J. Wang. Development of Closed-loop Control Strategy for Urea-SCR Based on NOx Sensors, *SAE papers* 2011-01-1324, 2011.

D. Y. Wand, S. Yao, M. Shost, J. Yoo, D. Cabush, and D. Racine. Ammonia Sensor for Closed-loop SCR Control, *SAE papers* 2008-01-0919, 2008.

J. Patchett, R. Verbeek, K. Grimston, G. Rice, J. Calabrese, and M. van Genderen. Control system for mobile NOx SCR applications, U.S. Patent 6 581 374, June, 2003.

D. Seher, M. Reichelt, and S. Wickert. Control Strategy for NOx - Emission reduction with SCR, *SAE papers* 2003-01-3362, 2003.

F. Willems, R. Cloudt, E. van den Eijnden, M. van Genderen, R. Verbeek, B. de Jager, W. Boomsma, and I. van den Heuvel. Is Closed-Loop SCR Control Required to Meet Future Emission Targets?, *SAE papers* 2007-01-1574, 2007.

A. Åberg, A. Widd, J. Abildskov, and J. K. Huusom. Estimation of Kinetic Parameters in an Automotive SCR Catalyst Model, *Topics in Catalysis* 59 (2016) 945-951.

A. Åberg, A. Widd, J. Abildskov, and J. K. Huusom. Parameter Estimation and Analysis of an Automotive Heavy-duty SCR Catalyst Model, *Chemical Engineering Science*, 161 (2017) 167-177.

K. J. Åström and M. Murray Feedback Systems: An Introduction for Scientists and Engineers, Princeton University Press, 2008, ISBN-10:0-691-13576-2.